

## **Low temperature oxidation of copper alloys - AEM and AFM characterization**

Mari Honkanen, Minnamari Vippola and Toivo Lepistö

Institute of Materials Science, Tampere University of Technology, P.O.B. 589, FIN-33101  
Tampere, Finland, email: [mari.honkanen@tut.fi](mailto:mari.honkanen@tut.fi)

## **Abstract**

Oxidation kinetics and oxide structures of three polycrystalline copper grades at different temperatures were studied by analytical transmission electron microscopy (AEM) and atomic force microscopy (AFM). The copper samples were oxidized in air at 200°C and 350°C for 1-1100 minutes. AEM and AFM studies indicated that alloying and increase of temperature, accelerated oxidation. At 200°C local oxidation was observed in the unalloyed copper samples while a uniform oxide layer formed on the alloyed coppers. At 350°C a uniform oxide layer formed on all copper samples. The oxide structure was nanocrystalline cubic Cu<sub>2</sub>O after all oxidation treatments at 200°C and after 5 minutes oxidation at 350°C. After 25 and 100 minutes oxidation at 350°C the crystal size of copper oxide had grown and the oxide structure was monoclinic CuO.

## **Keywords**

Analytical transmission electron microscopy (AEM), atomic force microscopy (AFM), copper alloy, copper oxidation, CuO, Cu<sub>2</sub>O

## 1. Introduction

Oxidation of metal and metal alloy surfaces plays a central role in many industrial applications. In general, the oxide film on the surface is either useful or undesirable depending on the application. At low temperatures the oxide film acts as a diffusion barrier protecting the metal from further oxidation. At higher temperatures oxidation can however continue due to diffusion through the oxide film [1]. The theory of the oxidation of metals by Cabrera and Mott describes oxide film formation on metals. According to the theory film grows at low temperatures as a uniform passivation layer based on internal electric field induced ion transport between the oxygen-oxide and oxide-metal interfaces. The ionic transport accelerates initial oxidation but is rapidly attenuated with increasing oxide film thickness [2]. Nowadays it is known that the theory of Cabrera-Mott is not absolutely correct to describe the oxidation process on metals. For example on copper the oxide film grows as oxide islands not as a uniform layer [1].

Oxidation of copper occurs via several stages: a complex chemisorption period with reconstruction followed by interfacial oxide nucleation, initial growth involving islands, coalescence and finally overlayer thickening [3]. The oxidation of copper surfaces starts with dissociation and chemisorption of oxygen on the copper. Chemisorped oxygen creates a Cu-O surface reconstruction. Further impinging oxygen molecules dissociate into oxygen atoms and then diffuse across the O-surface where they either re-evaporate, form a new oxide nuclei or are captured by existing nuclei. Due to that many small islands are formed at low temperatures. At elevated temperatures, however only few large islands are formed because of the higher movement of oxygen atoms and their the more probable attachment to existing islands than to form new ones. Oxide islands grow three-dimensionally into the substrate because the formation of oxide is accompanied with the conversion of copper atoms from the

substrate to oxide islands. The islands grow and coalesce as a function of oxygen. When the coalescence of the islands has completed and a uniform oxide layer covers the surface and the further growth is controlled by diffusion process through the oxide layer [4]. As soon as a thin continuous oxide film has formed on a metal surface the metal and gaseous reactants are spatially separated by a barrier and the reaction can continue only if cations, anions or both and electrons diffuse through the oxide layer [5]. J. Yang et al. have demonstrated that oxide film nucleates and grows as oxide islands not as a uniform layer even at atmospheric pressure [1, 5].

The crystallographic orientation of copper material has an effect on the nucleation behaviour, growth rate and the orientation of the oxide film. Young et al. determined the oxidation rates of different copper single crystal faces by measuring the increase in the oxide film thickness as a function of time. Measured faces were (100), (111), (110) and (311) and temperatures were 70, 106, 130, 159 and 178°C (1 atm). The relative order of decreasing oxidation rates was (100), (111), (110) and (311). Differences increased with temperature [6]. Zhou and Yang have explained the faster oxidation rate of Cu(100) to that of Cu(110) by the smaller path length of surface diffusion of oxygen on Cu(110) and larger surface energy of Cu(110) [4].

Depending on temperature and oxygen partial pressure, oxidation layer of copper consists Cu<sub>2</sub>O only or both Cu<sub>2</sub>O and CuO [7]. Thermodynamic calculations by Lawless and Gwathmey reveal that both Cu<sub>2</sub>O and CuO are stable throughout the entire ranges of pressure and temperature covered in their experiments (pressures between  $1 \times 10^{-3}$  and 1 atm and temperatures between 170 and 450°C) [8]. J. Li et al. have investigated the oxidation kinetics of the copper thin film at temperatures below 300°C in air. In these conditions two copper

oxides formed:  $\text{Cu}_2\text{O}$  and  $\text{CuO}$ . They found that copper was first oxidized to  $\text{Cu}_2\text{O}$  at  $200^\circ\text{C}$  and then to  $\text{CuO}$  at  $300^\circ\text{C}$  [9].

Lenglet et al. have obtained that low temperature oxidation ( $< 300^\circ\text{C}$ ) of copper can lead also to the formation of  $\text{Cu}_3\text{O}_2$  phase before of  $\text{CuO}$ . The experimental results for oxidation at  $300^\circ\text{C}$  indicate that the oxidation involves a fast process of  $\text{Cu}$  to  $\text{Cu}_3\text{O}_2$  and a slow process for the formation of  $\text{CuO}$ . This mechanism precedes the formation of a multiphase and multilayer structure  $\text{CuO}/\text{Cu}_3\text{O}_2/\text{Cu}_2\text{O}/\text{Cu}$ .  $\text{CuO}$  may be obtained oxidation of  $\text{Cu}_2\text{O}$  or  $\text{Cu}_3\text{O}_2$  [10, 11, 12, 13]:



or [10]:



or by the dissociation of  $\text{Cu}_3\text{O}_2$  [10] or  $\text{Cu}_2\text{O}$  [12]:



S. Ghosh et al. have found out that when temperature is  $200^\circ\text{C}$  or higher,  $\text{Cu}_2\text{O}$  starts reacting with oxygen and  $\text{CuO}$  phase starts to form according to equation (1) [13]. Lattice plane

spacing values (d values) for  $\text{Cu}_2\text{O}$ ,  $\text{CuO}$  and  $\text{Cu}_3\text{O}_2$  from literature are presented in Tab. 1 [10, 14].

A. Brazdeikis et al. have studied the formation of thin copper oxide ( $\text{CuO}$ ) films on  $\text{MgO}(100)$  by reflection high-energy electron diffraction (RHEED) and atomic force microscopy (AFM). The  $\text{CuO}$  films were grown by molecular beam epitaxy using  $\text{NO}_2$  as oxidant and copper was evaporated from a Knudsen effusion cell. Their AFM images and line profiles show changes in the surface morphology as the thickness of  $\text{CuO}$  layer increases.  $\text{CuO}$  islands having a round shape nucleated randomly onto the  $\text{MgO}$  surface. The lateral dimensions of islands were larger than vertical ones indicating that  $\text{CuO}$  grew laterally more rapidly. Further deposition at the surface led to the increase of the number and size of  $\text{CuO}$  islands, and also to the appearance of a large number of pits in the film [15]. S. Ghosh et al. also studied copper oxides with AFM. They deposited  $\text{Cu}_2\text{O}$  and  $\text{CuO}$  films by reactive sputtering at different substrate temperatures. Their studies indicated that  $\text{Cu}_2\text{O}$  phase is prominent at temperatures up to  $150^\circ\text{C}$  and  $\text{CuO}$  phase was obtained at  $300^\circ\text{C}$ . Based on their AFM studies, they concluded that at the beginning when temperature was raised, the grain size of the oxide increased but at  $300^\circ\text{C}$  the grain size decreased. Due to that they assumed that the reduction in grain size could be attributed to the crystallographic phase change from  $\text{Cu}_2\text{O}$  to  $\text{CuO}$  [13].

The aim of this work was to study oxidation kinetics of three different polycrystalline copper grades and characterize their oxide structure at different temperatures (1 atm) by analytical transmission electron microscopy (AEM) and atomic force microscopy (AFM). In this work, oxidation treatments were made in air at  $200^\circ\text{C}$  and  $350^\circ\text{C}$  with industrial polycrystalline copper grades provided by Outokumpu Copper.

## 2. Experimental

In this work three different copper grades were studied: unalloyed OF-copper (oxygen free, oxygen content <5 ppm), CuAg-copper (silver bearing, Ag ~ 0.5 - 2 wt-%) and DHP-copper (phosphor deoxidised copper, P 0,013-0,050 wt-%). CuAg-copper was specially made for oxidation studies. This alloy was not a standard quality. Due to the unoptimized processing conditions it's silver content varied in the as-received test material.

The test materials were received in the cold rolled condition (reduction 80 - 90 %). A microstructure of the cold rolled material was heterogenous and therefore more homogenous microstructures for the oxidation treatments were produced by recrystallization treatment. Recrystallization temperature for each copper grade was defined by annealing samples at different temperatures for two hours and measuring the resulting Vickers-hardness values. Based on these studies the recrystallization temperature of OF-copper was selected as 350°C, CuAg-copper 225°C and DHP-copper 450°C. The average grain size of all test samples after recrystallization was 5 µm.

The oxidation treatments were carried out in a ceramic furnace in air at 200°C and 350°C. Oxidation times varied from 1 to 1100 minutes depending on the material and oxidation temperature. AEM samples for the oxidation treatments were prepared with Tenupol 5 twin jet electrolytical polisher using a solution of nitric acid in methanol (1:2) at -50°C. Pre-thinning before electropolishing was made mechanically with SiC-papers to 0.1 mm thickness and then 3 mm diameter discs were cut from the prethinned samples. After oxidation treatments at 350° C samples were ion milled from the backside with Gatan Precision Ion Polishing System 691 (PIPS). Samples for AFM studies were cut into the size of 5 mm x 5

mm. After cutting and mechanical grinding, the samples were polished with Beaker Method [16] using the same solution as with the electrolytic polishing of the AEM samples.

The fresh and oxidized samples were studied with AEM (Model Jeol JEM 2010 equipped with Noran Vantage EDS-system) and with AFM (Nanoscope II AFM, Digital Instruments). In AEM studies the same area of the sample was located and beam direction  $\mathbf{B} \approx [0,1,1]$  was used in photographing after each oxidation treatment at 200°C. Oxidation treatments at 350°C led to a situation where it was impossible to study the same areas as ion milling had modified the samples so much that the same areas could not be recognized. The fresh and oxidized AEM samples were characterized by imaging, SAED and EDS analyses. In AFM studies the same sample was oxidized many times using different exposure periods at a certain temperature. Before and between oxidation treatments the sample was studied with AFM using a pyramidal probe and a 200  $\mu\text{m}$  long triangular cantilever made of silicon nitride with a spring constant of 0.12 N/m. Contact and constant force modes were used. Root-mean-square (rms) surface roughness values of the samples were calculated from AFM images (2  $\mu\text{m}$  x 2  $\mu\text{m}$ ) with the support of software.

### **3. Results and discussion**

In this research oxidation kinetics, oxide structures and morphology of three copper grades were studied with AEM and AFM. Oxidation treatments were carried out at 200°C and 350°C.



### 3.1. *Structure of copper oxide at 200 °C*

AEM images and electron diffraction patterns of OF-, CuAg- and DHP-copper samples before and after oxidation treatment at 200°C are presented in Fig 1. Different kinds of areas were detected in the unalloyed OF-copper sample after oxidation at 200°C. On some areas (dark area in TEM image) electron diffraction patterns indicated that even after 100 minutes oxidation almost the same structure as in the fresh copper existed. In the other areas (bright area in TEM image) electron diffraction pattern indicated a copper oxide structure. This kind of variation was not observed in the alloyed CuAg- and DHP-copper samples. This indicates that the oxide layer on OF-copper is discontinuous. On the other hand a more or less uniform oxide layer is covering CuAg- and DHP-copper samples. Due to the discontinuous nature of the oxide layer in OF-copper sample after 100 minutes treatment they were oxidized also for 200 and 1100 minutes at 200°C. After 200 minutes of oxidation the situation was the same as after 100 minutes. However, after 1100 minutes oxidation AEM analyses indicated existence of a uniform oxide layer. This correlates well with Yang's et al. studies demonstrating that the oxide layer nucleates and grows even at atmospheric pressure as oxide islands not as a uniform layer [1, 5]. In this work, local oxidation was detected only with OF-copper. In CuAg- and DHP-copper alloying elements accelerated forming of the uniform oxide layer because the continuous oxide layer was detected already after 25 minutes oxidation in these alloyed coppers.

Electron diffraction patterns of OF-, CuAg- and DHP-copper samples taken before and after each oxidation treatment (5, 25 and 100 minutes) at 200°C are presented in Fig. 2. They indicate that oxidation starts between 5 and 25 minutes oxidation. As mentioned earlier on the OF-copper samples there were variations on the oxide structure after 25 and 100 minutes

oxidation. The structures of the copper oxides were determined from electron diffraction patterns. All electron diffraction patterns indicated the nanocrystalline structure of the copper oxide. The calculated d values corresponded closely to d values for cubic Cu<sub>2</sub>O ( $a \approx 0.427$  nm) [14]. This result agreed well with those presented in the literature where it was found that depending on the temperature, the oxidation layer of the copper consists Cu<sub>2</sub>O only or both Cu<sub>2</sub>O and CuO [7] and that the copper oxidizes first to Cu<sub>2</sub>O at low temperatures [9].

### 3.2. *Structure of copper oxide at 350 °C*

AEM images and electron diffraction patterns of OF-, CuAg- and DHP-copper samples are presented in Fig. 3 before and after oxidation at 350°C. Electron diffraction patterns of OF-, CuAg- and DHP-copper samples are presented in Fig. 4 before and after each oxidation treatment (1, 5, 25 and 100 minutes) at 350°C. They indicated that oxidation started between 1 and 5 minutes oxidation. The uniform oxide layer was formed on all copper grades at 350°C after 5 minutes exposure. Electron diffraction patterns indicated the nanocrystalline structure of the copper oxide after 5 minutes oxidation and the calculated d values corresponded closely to d values for cubic Cu<sub>2</sub>O [14]. After 25 and 100 minutes oxidation electron diffraction patterns differed significantly from those taken after 5 minutes oxidation. Patterns indicated that the crystal size of the oxide had grown. Instead of clear ring patterns separated spots could be seen. The calculated d values corresponded close to d values for monoclinic CuO ( $a \approx 4.69$ ,  $b \approx 3.42$ ,  $c \approx 5.13$  and  $\beta = 99.51^\circ$ ) [14]. There might be Cu<sub>2</sub>O layer under CuO layer but rings or spots of Cu<sub>2</sub>O were so weak that it was very difficult to see them. Therefore more detailed studies are needed, for example by studying cross-sectional oxidized copper samples. Again, the results of the present study agreed well with earlier studies where it was shown

that copper was first oxidized to  $\text{Cu}_2\text{O}$  at  $200^\circ\text{C}$  and then to  $\text{CuO}$  at  $300^\circ\text{C}$  [9] and that formation of  $\text{Cu}_2\text{O}$  is a fast process and  $\text{CuO}$  forms much more slowly [10].

### 3.3. *Oxidation rates at $200^\circ\text{C}$ and $350^\circ\text{C}$*

The effect of temperature and alloying elements on the oxidation rates was also studied. The average oxygen contents of OF-, CuAg and DHP-copper samples were determined as a function of time after oxidation treatments at  $200^\circ\text{C}$  and  $350^\circ\text{C}$  (Fig. 5). At the lower temperature alloying elements accelerated oxidation more than at the higher temperature. At  $350^\circ\text{C}$  oxidation rates of different copper grades were more close to each other than at  $200^\circ\text{C}$ . It should be noted that after oxidation at  $350^\circ\text{C}$  only the backside of sample was ion milled and it will have an effect on the measured oxygen contents. However in general, increase of temperature and addition of alloying elements accelerated oxidation. Oxygen content measurements indicated the same phenomena as electron diffraction patterns: significant oxidation starts to happen during 25 minutes oxidation. Oxidation rates decreased after 25 minutes and oxygen contents saturated at  $200^\circ\text{C}$  to  $\sim 30$  at% and at  $350^\circ\text{C}$  to  $\sim 50$  at%. This correlates well to the results of G. Zhou and J. Yang who have observed that as soon as the coalescence of the oxide islands has completed there is reduction in the growth rate of the oxide due to the change of the oxidation from a surface diffusion controlled process to the bulk diffusion controlled one. The self-limiting oxidation is due to the coalescence of the islands what switches off the surface diffusion route and requires slower bulk diffusion for further oxidation [4].

### 3.4. *Morphology of copper oxides*

Fresh and at 200°C and at 350°C oxidized samples were studied with AFM. Images, measured rms roughness values and line profiles showed significant changes in the surface morphology during the oxidation treatments. AFM studies indicated that the temperature, exposure time and alloying elements effected on the surface morphology. Like AEM studies also AFM studies illustrated that remarkable oxidation started at 200°C between 5 and 25 minutes and at 350°C between 1 and 5 minutes. In these oxidation time ranges morphology changed and the surface roughness increased prominently. Based on AFM studies, the oxides grew randomly and homogeneously on the surfaces and due to that the formed oxide layers were continuous. Line profiles showed that the oxides are fairly elliptical in shape and that oxides were more pointed in shape after treatment at 350°C than at 200°C. The microscopically discontinuous nature of the oxide layer on OF-copper at 200°C could not be seen by AFM imaging like by AEM studies. However, the effect of the alloying elements on the oxidation could be seen also in AFM studies. The surface roughness of alloyed coppers increased faster during the oxidation treatments than that of the unalloyed copper. AFM images and line profiles indicated that the grain size of oxides increased with increasing temperature and exposure time, just like also A. Brazdeikis et al. [15] and S. Ghosh [13] et al. have noticed during their studies. AFM images of the fresh and at 200°C and at 350°C oxidized OF-copper are presented in Fig. 7. Rms roughness values of the fresh and oxidized copper samples are presented in table 2.

#### 4. Conclusions

In this work, oxidation behaviour of unalloyed OF-copper and alloyed CuAg- and DHP-copper was studied. Recrystallized copper samples were oxidized in air at 200°C and 350°C. In general, alloying and higher temperature accelerated oxidation. AEM and AFM studies indicated that samples had oxidized after 25 minutes at 200°C and at 350°C oxidation had happened already after 5 minutes oxidation. At 200°C oxygen content of OF-copper varied what indicates that the oxidation of OF-copper at 200°C started locally and only after the long term oxidation and at higher temperature the uniform oxide layer was formed. At 200°C after all oxidation treatments and at 350°C after 5 minutes oxidation the oxide structure was nanocrystalline cubic Cu<sub>2</sub>O. After 25 and 100 minutes oxidation at 350°C the crystal size of the oxide had grown and the oxide structure was monoclinic CuO. Possible Cu<sub>2</sub>O layer under CuO layer was difficult to detect. AFM images and rms roughness values showed significant changes in the surface morphology during oxidation. Alloying elements accelerated oxidation because the surface roughness of alloyed coppers increased faster during oxidation than that of the unalloyed copper.

## **Acknowledgements**

The authors thank The National Technology Agency of Finland (TEKES) for financial support.

## References

1. J. YANG et al., *Applied Physics Letters* 73 (1998) 2841.
2. N. CABRERA and N. MOTT, *Reports on Progress in Physics* 12 (1948) 163.
3. D. COCKE et al., *Applied Surface Science* 84 (1995) 153.
4. G. ZHOU and J. YANG, *Surface Science* 531 (2003) 359.
5. K. LAWLESS, *Reports on Progress in Physics* 37 (1974) 231.
6. F. YOUNG, J. CATHCART and A. GWATHMEY, *Acta Metall.* 4 (1956) 145.
7. U. ANIEKWE and T. UTIGARD, *Canadian Metallurgical Quarterly* 38 (1999) 277.
8. K. LAWLESS and A. GWATHMEY, *Acta Metallurgica* 4, (1956) 153.
9. J. LI, J. MAYER and E. COLGAN, *Journal of Applied Physics* 70 (1990) 2820.
10. M. LENGLET et al., *Materials Research Bulletin* 30 (1995) 393.
11. N. BELLAKHAL et al., *Materials Science and Engineering B41* (1996) 206.
12. A. MUSA, T. AKOMOLAFE and M. CARTER, *Solar Energy Materials and Solar Cells* 51 (1998) 305.
13. S. GHOSH et al. *Vacuum* 57 (2000) 377.
14. International Centre for Diffraction Data (ICDD), *Powder Diffraction File Database* 1999.
15. A. BRAZDEIKIS, U. KARLSSON and A. FLODSTRÖM, *Thin Solid Films* 281-282 (1996) 57.
16. B. KESTEL, *Polishing methods for metallic and ceramic transmission electron microscopy specimens*, Argonne National Laboratory, Materials Science Division, Illinois 1981, 58 p.

## Table captions

Table 1. D values from literature for  $\text{Cu}_2\text{O}$ ,  $\text{CuO}$  and  $\text{Cu}_3\text{O}_2$  [10, 14].

Table 2. Rms surface roughness values in nanometers of the fresh and oxidized coppers.

## Figure captions

Figure 1. AEM images and electron diffraction patterns of OF- (a), CuAg- (b) and DHP-copper (c) before (upper) and after (lower) oxidation (100 min.) at  $200^\circ\text{C}$ .

Figure 2. Electron diffraction patterns of (a) OF-, (b) CuAg- and (c) DHP-copper samples before and after each oxidation treatment at  $200^\circ\text{C}$ .

Figure 3. TEM-images and electron diffraction patterns of OF- (a), CuAg- (b) and DHP-copper (c) before (upper) and after (lower) oxidation treatments (100 min.) at  $350^\circ\text{C}$ .

Figure 4. Electron diffraction patterns of (a) OF-, (b) CuAg- and (c) DHP-copper samples before and after oxidation treatment at  $350^\circ\text{C}$ .

Figure 5. Oxidation of OF-, CuAg and DHP-copper at 200 and  $350^\circ\text{C}$ .

Figure 6. Oxidation of OF-copper at  $200^\circ\text{C}$ . Dashed perpendicular lines indicate min. and max. values of oxygen content.

Figure 7. AFM images of fresh and oxidized OF-copper (a) fresh sample (b) oxidized at  $200^\circ\text{C}$  for 5,25 and 100 min. and (c) oxidized at  $350^\circ\text{C}$  for 1, 5 and 100 min.



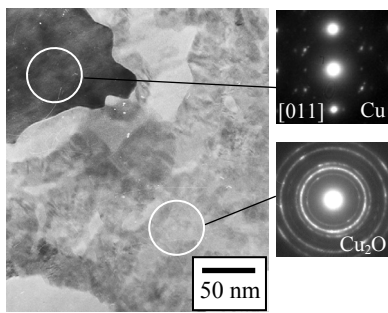
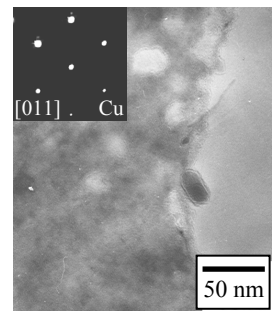
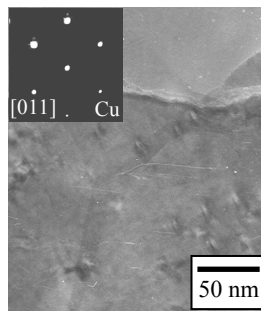
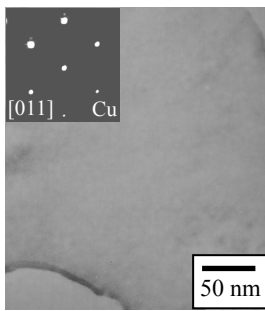
**Table 1.**

(hkl)	d [nm] Cu <sub>2</sub> O [ref. 14]	d [nm] CuO [ref. 14]	d [nm] Cu <sub>3</sub> O <sub>2</sub> [ref. 10]
1,1,0	0.302	0.275	0.308
0,0,2	-	0.253	-
1,1,-1	-	0.252	-
1,1,1	0.247	0.232	0.249
2,0,0	0.214	0.231	0.217
0,2,2	-	0.142	-
2,2,0	0.151	0.138	0.152
3,1,1	-	0.129	-

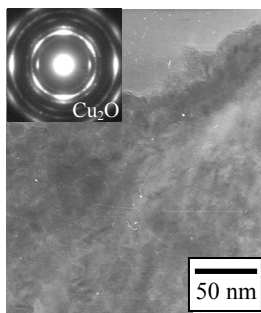
**Table 2.**

<b>Oxidation temperature [°C]</b>	Fresh	200°C			350°C			
<b>Oxidation time [min]</b>		5 min.	25 min.	100 min.	1 min.	5 min.	25 min.	100 min.
<b>OF (Rms [nm])</b>	0.5	2	4	8	1	4	26	33
<b>CuAg (Rms [nm])</b>	1.0	1	4	8	2	5	36	36
<b>DHP (Rms [nm])</b>	1.0	2	3	9	2	2	14	48

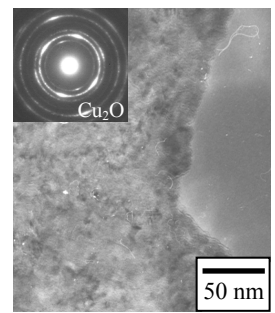
**Figure 1.**



(a)



(b)



(c)

Figure 2.

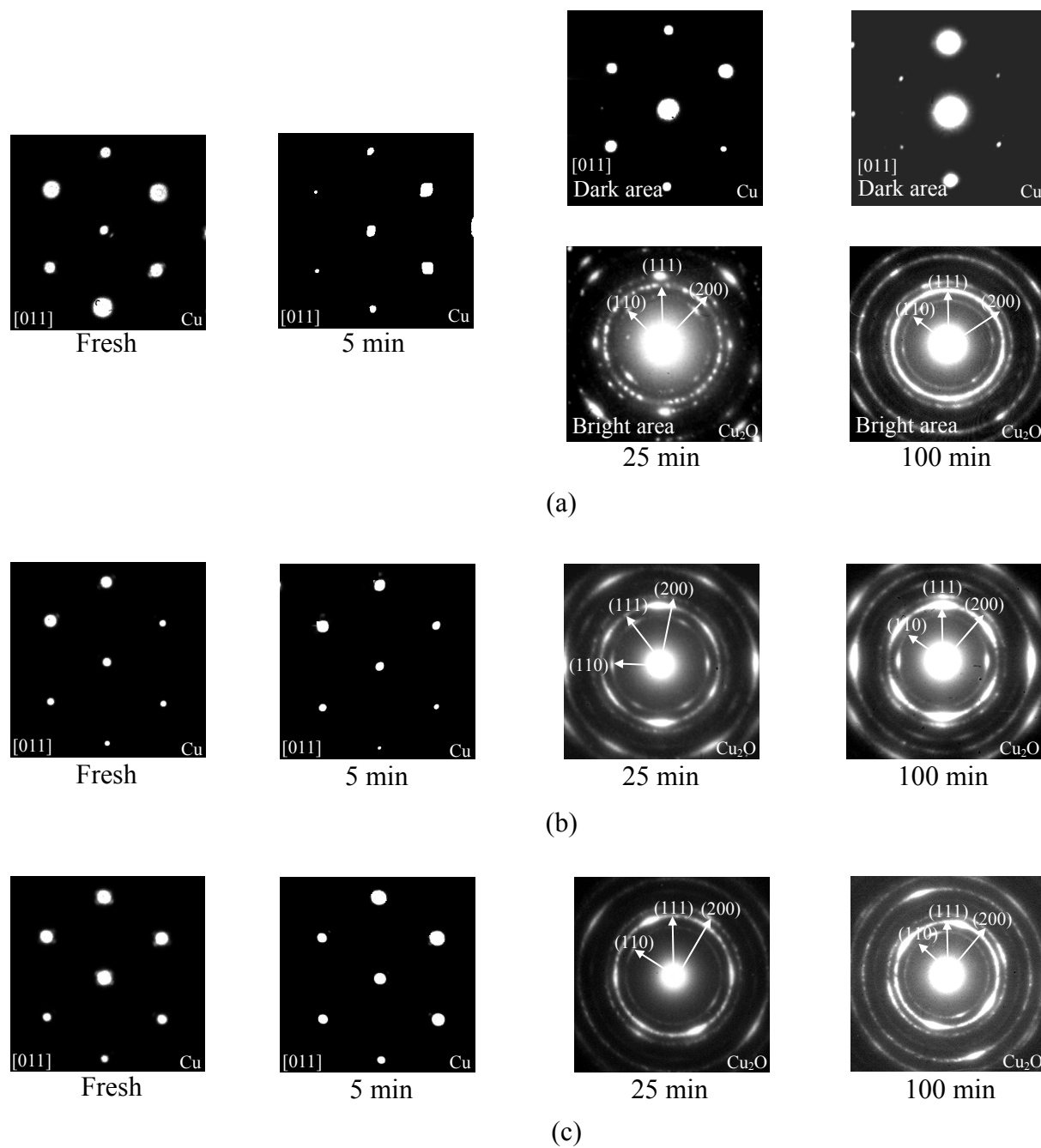
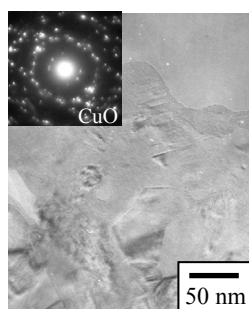
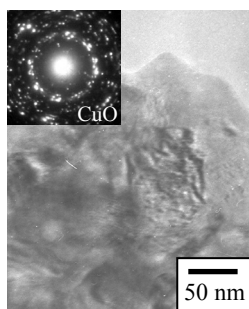
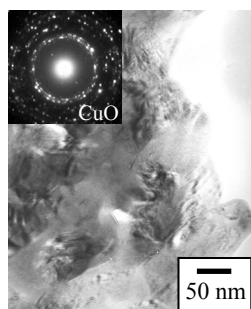
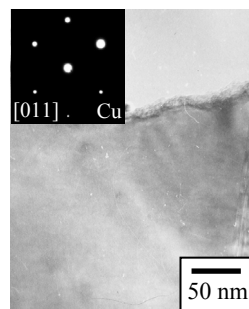
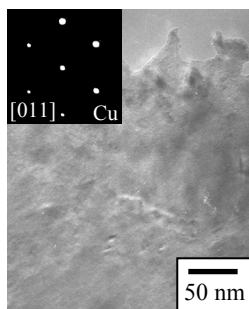
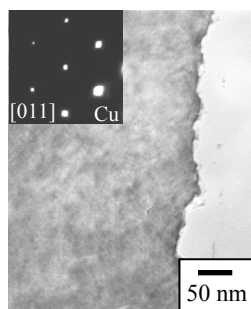


**Figure 3.**



(a)

(b)

(c)

Figure 4.

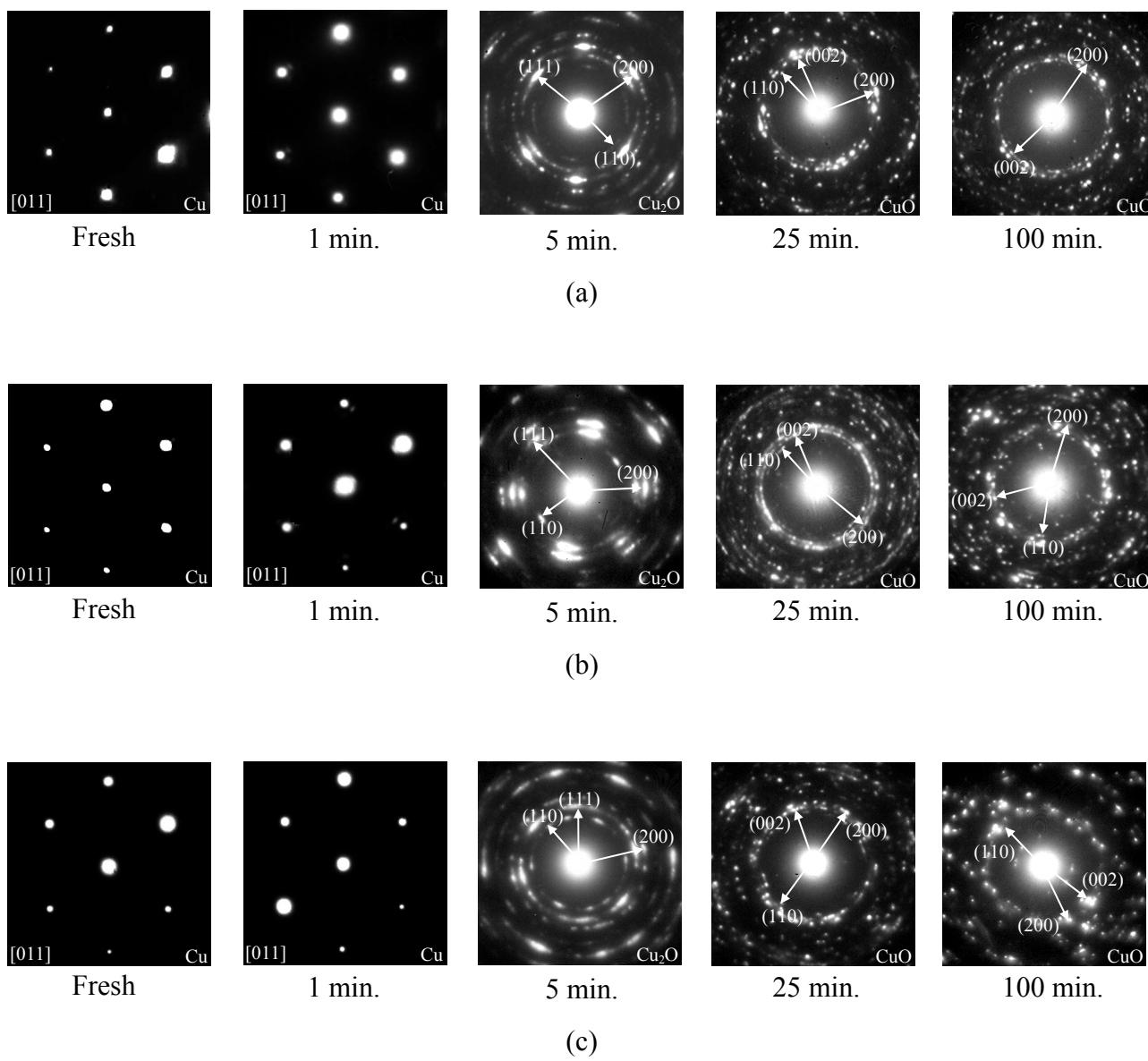


Figure 5.

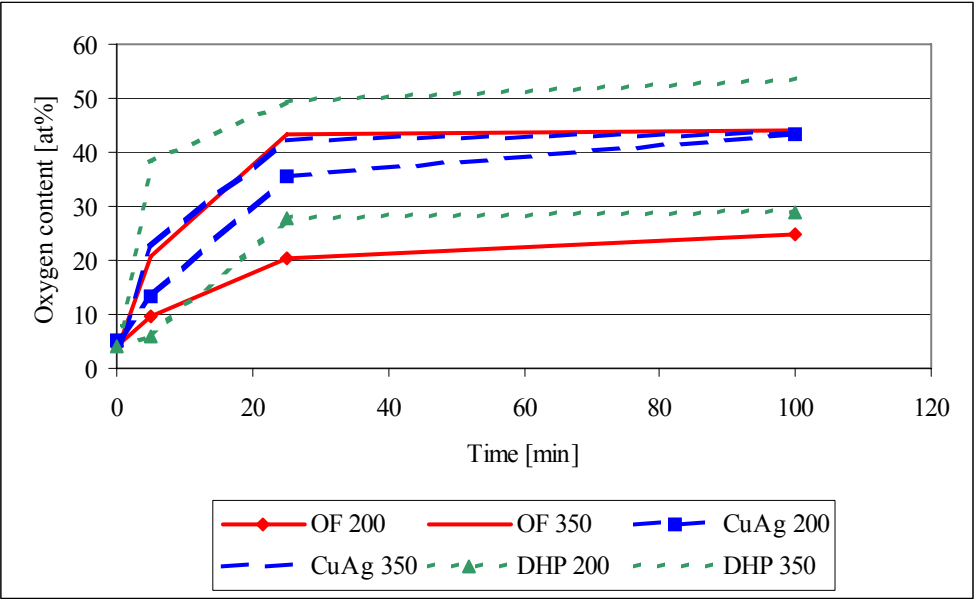


Figure 6.

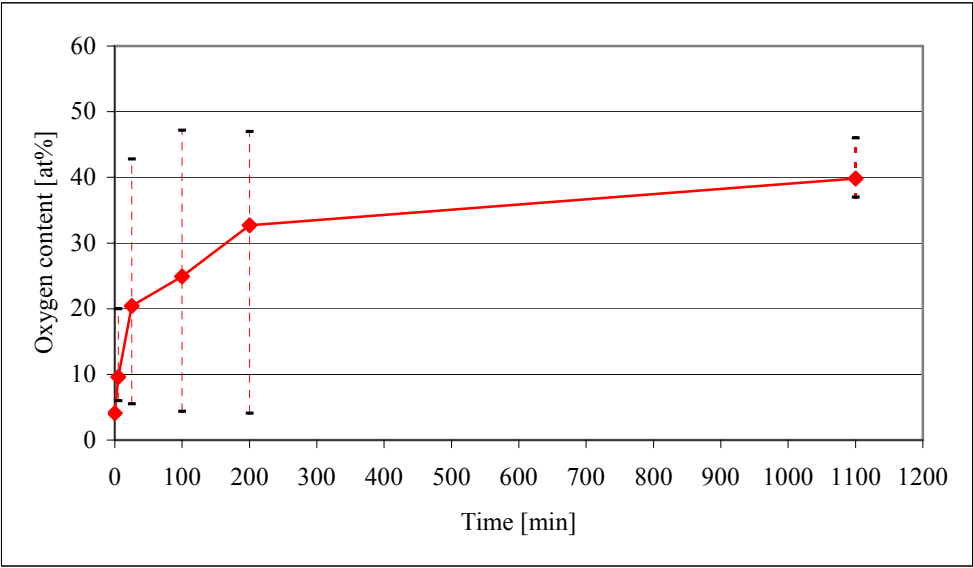




Figure 7.

